DNA barcoded peptide-MHC multimers to measure and monitor minor histocompatibility antigen-specific T cells after allogeneic stem cell transplantation

Kyra J Fuchs [1], Marcus Göransson,[2] Michel G D Kester,[1] Natasja W Ettienne,[2] Marian van de Meent,[1] Rob C M de Jong,[1] Eva A S Koster [1], Constantijn J M Halkes,[1] Ferenc Scheeren [3], Mirjam H M Heemskerk [1], Peter van Balen,[1] J H Frederik Falkenburg,[1] Sine R Hadrup [2], Marieke Griffioen[1]

¹Department of Hematology, Leiden University Medical Center, Leiden, The Netherlands
²Department of Health Technology, Technical University of Denmark, Lyngby, Denmark
³Department of Dermatology, Leiden University Medical Center, Leiden, The Netherlands

Correspondence to
Dr Marieke Griffioen;
m.griffioen@lumc.nl

ABSTRACT

Allogeneic stem cell transplantation (alloSCT) provides a curative treatment option for hematological malignancies. After HLA-matched alloSCT, donor-derived T cells recognize minor histocompatibility antigens (MiHAs), which are polymorphic peptides presented by HLA on patient cells. MiHAs are absent on donor cells due to genetic differences between patient and donor. T cells targeting broadly expressed MiHAs induce graft-versus-leukemia (GvL) reactivity as well as graft-versus-host disease (GvHD), while T cells for MiHAs with restricted or preferential expression on hematopoietic or non-hematopoietic cells may skew responses toward GvL or GvHD, respectively. Besides tissue expression, overall strength of GvL and GvHD is also determined by T-cell frequencies against MiHAs.

Here, we explored the use of DNA barcode-labeled peptide-MHC multimers to detect and monitor antigen-specific T cells for the recently expanded repertoire of HLA-I-restricted MiHAs. In 16 patients who experienced an immune response after donor lymphocyte infusion, variable T-cell frequencies up to 30.5% of CD8⁺ T cells were measured for 49 MiHAs. High T-cell frequencies above 1% were measured in 12 patients for 19 MiHAs, with the majority directed against mismatched MiHAs, typically 6–8 weeks after donor lymphocyte infusion and at the onset of GvHD. The 12 patients included 9 of 10 patients with severe GvHD, 2 of 3 patients with limited GvHD and 1 of 3 patients without GvHD.

In conclusion, we demonstrated that barcoded peptide-MHC multimers reliably detect and allow monitoring for MiHA-specific T cells during treatment to investigate the kinetics of immune responses and their impact on development of GvL and GvHD after HLA-matched alloSCT.

BACKGROUND

Allogeneic stem cell transplantation (alloSCT) provides a curative treatment option for patients with hematological malignancies by establishing immune responses against malignant cells. However, this graft-versus-leukemia (GvL) effect is often accompanied by graft-versus-host disease (GvHD) impacting the morbidity and survival of

WHAT IS ALREADY KNOWN ON THIS TOPIC

⇒ After HLA-matched allogeneic stem cell transplantation, donor T cells targeting minor histocompatibility antigens (MiHAs) can induce the therapeutic graft-versus-leukemia (GvL) effect, but also potentially life-threatening graft-versus-host disease (GvHD).

⇒ Patients have previously been monitored for MiHA-specific T cells, but the repertoire of HLA class I-restricted MiHAs was far from complete, limiting accurate analysis of the strength, kinetics, breadth, and specificity of MiHA-specific T-cell responses that drive GvL and GvHD.

⇒ The dominant repertoire of HLA class I-restricted MiHAs has recently been mostly discovered for five common HLAs and enables monitoring large patient cohorts for detailed analysis of MiHA-specific T-cell responses.

WHAT THIS STUDY ADDS

⇒ By screening 16 transplanted patients, DNA barcoded peptide-MHC multimer screening proved to be a feasible method to detect CD8+ T cells against a large number of MiHAs.

⇒ The landscape of MiHAs is targeted by a vast range of T-cell frequencies from barely detectable to 30.5% of CD8+ T cells, illustrating immunodominance among MiHAs.

HOW THIS STUDY MIGHT AFFECT RESEARCH, PRACTICE OR POLICY

⇒ DNA barcoded peptide-MHC multimer screening is a feasible method to investigate MiHA-specific T-cell responses in large patient cohorts.

⇒ Analyzing MiHA-specific T-cell responses in patients with different clinical outcomes across transplantation protocols will give detailed insight into the immune responses that drive GvL and GvHD, which is relevant for treatment optimization and clinical decision-making before and after allogeneic stem cell transplantation.

patients. The GvL effect is caused by alloreactive donor T cells targeting hematopoietic patient cells, including malignant cells,

whereas GvHD is orchestrated by donor T cells attacking patients' healthy non-hematopoietic tissues.[1] To reduce the risk and severity of GvHD while preserving GvL reactivity, patients can be treated with T cell-depleted alloSCT followed by postponed pre-emptive or prophylactic donor lymphocyte infusion (DLI).[2] While DLI administration after alloSCT can initiate the GvL effect and thereby reduce the risk of relapse, it can still cause significant GvHD.[3]

After HLA-matched alloSCT, donor T cells target minor histocompatibility antigens (MiHAs) which are polymorphic peptides presented on patient cells by HLA molecules.[4] These antigens are foreign to donor T cells due to genetic differences between patient and donor.[5] Depending on the tissue distribution of MiHAs, T cells targeting broadly expressed MiHAs can cause GvL reactivity as well as GvHD, while donor T cells specific for MiHAs that are restricted to hematopoietic or non-hematopoietic cells may skew responses toward GvL or GvHD, respectively.

Previous studies attempted to explore the impact of MiHAs on GvL and GvHD in large patient cohorts by measuring total SNP mismatches in patient-donor pairs, selected SNP mismatches for predicted MiHAs or small sets of identified MiHAs.[6–11] However, SNP mismatches or predicted MiHAs do not warrant actual surface presentation by HLA[12] or peptide recognition by donor T cells.[13] Peptides may be inefficiently processed, cleaved intracellularly, or the difference between the MiHA and its allelic variant may be small and remain unnoticed by donor T cells.[5] The donor T-cell repertoire may also lack MiHA-specific T-cell receptors, or the immune response after alloSCT may be dominated by T cells targeting other MiHAs. Therefore, research to investigate the effect of MiHAs on GvL or GvHD falls short if solely based on SNP mismatches or predicted MiHAs due to many false positives.

To understand and manipulate the development of GvL and GvHD, it is crucial to measure and monitor patients for immune responses to determine the presence, strength, and dominance of T cells against individual MiHAs after HLA-matched alloSCT. This may enable predictions on therapy outcome, a more directed donor selection, or manipulation of immune responses by infusion or depletion of antigen-specific T cells. We recently expanded the repertoire of HLA class I-restricted MiHAs to a total of 159 antigens and showed in a cohort of 39 patients that 64% of isolated MiHA-specific T-cell clones were directed against recurrent MiHAs targeted in multiple patients.[14] With each included patient, discovery of new antigens declined, suggesting that the dominant repertoire of HLA class I-restricted MiHAs that are frequently mismatched in the European population has probably been largely discovered for five common HLAs (HLA-A*01:01, A*02:01, A*03:01, B*07:02, B*08:01).[14] These MiHAs are now available to validate their relevance for T-cell monitoring to measure and follow GvL and GvHD responses in independent patient cohorts

after various alloSCT therapeutic approaches. However, measuring T-cell frequencies by conventional fluorescent peptide-major histocompatibility complex (pMHC) tetramer staining is tedious and challenging due to the high number of potential targets per patient. Furthermore, patient sample availability is restricted, requiring a method that reliably works with limited volume of patient peripheral blood. Here, we present a potential solution using DNA barcode-labeled pMHC-multimers that enables simultaneous screening for a large number of peptide targets.[15 16]

In this study, we set out to investigate the potential of barcode-labeled pMHC-multimer screening to measure frequencies of MiHA-specific T cells by screening 16 patients who responded to DLI after HLA-matched T-cell depleted alloSCT. We demonstrated that barcoded pMHC-multimers can be used to detect and follow MiHA-specific T cells in large patient cohorts, which is essential to investigate the impact of MiHAs on development of GvL and GvHD after alloSCT.

METHODS

Patient material
Peripheral blood mononuclear cells (PBMCs) and bone marrow mononuclear cells (BMMCs) from 16 patients who were previously screened for MiHA identification[14] and healthy third-party donors (central blood bank at Rigshospitalet, Copenhagen) were isolated by Ficoll-Isopaque centrifugation and cryopreserved.

Peptide production and modification
Peptides were synthesized in-house or by Pepscan (purity >70%) and dissolved in DMSO to a concentration of 10 mM. Peptides containing cysteines were cysteinylated or reduced using Dithiothreitol (DTT). Peptides were diluted in 50 mM ammonium bicarbonate at pH 8 to a concentration of 1 mM. DTT was added to a final concentration of 2 mM and the sample incubated for 15 min at 50°C. For cysteinylation, cysteine and hydrogen peroxide were added to concentrations of 10 mM and 15 mM, respectively, and samples were incubated for 30 min at room temperature (RT).

Production of pMHC-monomers
Recombinant heavy chains and human β2 microglobulin light chains of HLA-A*01:01, HLA-A*02:01, HLA-A*03:01, HLA-A*24:02, HLA-B*07:02, HLA-B*08:01, HLA-B*35:01, B*40:01, C*03:03, C*03:04, C*07:01, and C*07:02 were produced in *Escherichia coli*. HLA chains were refolded in the presence of UV-sensitive ligands[17–21] or redox-refolded, purified, and biotinylated, as previously described.[22] Stabilized HLA-A*02:01 was folded and purified empty, as previously described.[23]

Generation of barcode-labeled pMHC-multimers
Barcode-labeled pMHC-multimers were produced as previously described.[15 21] Briefly, oligonucleotides (LGC

Biosearch Technologies) with distinct 25-mer nucleotide sequences[24] and additional six nucleotides as unique molecular identifier[25] with a conjugated 5' biotin tag (oligo A's) were annealed to partially complementary oligonucleotides (oligo B's). The annealed oligos A and B were elongated, creating unique combinations of double-stranded AxBy DNA barcodes. These barcodes were attached to dextran backbones (Fina Biosolutions) conjugated with streptavidin and phycoerythrin (PE) or allophycocyanin (APC). Barcoded dextran-conjugates were incubated with pMHC-monomers and assembled pMHC-multimers were stored −20°C in freezing buffer (phosphate-buffered saline (PBS), 0.5% bovine serum albumin (BSA), 100 µg/mL herring DNA, 2 mM EDTA, 5% Glycerol and 909 nM D-biotin).

Structural validation of pMHC-complexes

K562 cells transduced with LILRB1 were cultured in Iscove's Modified Dulbecco's Medium (IMDM) supplemented with 10% FBS (Bodinco), 1.5% glutamine (200 mM; Lonza) and 1% penicillin/streptomycin (200 mM; Lonza). LILRB1 only binds to stable pMHC-complexes. For structural validation of conventional pMHC-complexes, 50,000 cells were stained with 1 µL of the pMHC-product in a volume of 25 µL and incubated for 15 min at 37°C. For validation of peptides in stabilized HLA-A*02:01, 1.5 µL of pMHC-complexes were incubated with 2 µL of a peptide labeled with fluorescein isothiocyanate (FITC) (FLPSDC(FITC)FPS)[26] for 30 min before incubation with 50,000 cells for 10 min at RT for competition between peptides. After washing, samples were measured by flow cytometry. The stability of pMHC-complexes was indicated by PE-positive K562 cells or PE-positive and FITC-negative K562 for conventional and stabilized pMHC-complexes, respectively.

Sorting of antigen-specific T cells

PBMCs were thawed, washed in RPMI-1640 (Fischer Scientific) with 10% FBS (Gibco) and resuspended in barcode-cytometry buffer (PBS with 0.5% BSA, 100 µg/mL herring DNA, 2 mM EDTA). Barcode-labeled pMHC-multimers were pooled for HLAs expressed in the respective patients. Aliquots of 5 µL from each pMHC-multimer pool were used as baseline for DNA barcode analysis. To inhibit non-specific binding of KIR^{+} T cells to HLA-C molecules, cells were blocked with anti-CD158 (KIR2DL1/S1/S3/S5) (BioLegend 339502) for 15 min in 25 µL, in the presence of 50 nM dasatinib to inhibit TCR downregulation, internalization and pMHC-multimer-induced cell death.[27] Subsequently, samples were incubated with pMHC-multimer pools for 30 min at RT and stained with CD3-BUV737 (BD 612753, dilution 1:200), CD8-BV480 (BD 566121, dilution 1:100), CD4-PE-Cy7 (BD 560649, dilution 1:200), CD14-FITC (BD 345784, dilution 1:33), CD19-FITC (BD 345776, dilution 1:15), CD16-FITC (BD 335035, dilution 1:66), and a dead cell marker (LIVE/DEAD Fixable Near-IR; Fisher Scientific L34976, dilution 1:1000) in 100 µL for 30 min on ice.

Cells were washed three times with barcode-cytometry buffer and fixated with 1% PFA for approximately 18 hours, resuspended in barcode-cytometry buffer and sorted within 2 days after staining. For each experiment, Fluorescence Minus One controls were included. T cells positive for CD3, CD8 and pMHC-multimers were sorted on FACSAria Fusion instruments into BSA-saturated tubes containing 50 µL barcode-cytometry buffer. PE-conjugated pMHC-multimer[+] and APC-conjugated pMHC-multimer^{+} cells were sorted into separate tubes. Sorted cell pellets were stored at −20°C.

DNA barcode amplification

DNA barcodes from sorted pMHC-multimer^{+} CD8^{+} T cells were amplified using Taq PCR Master Mix Kit (QIAGEN) and 3 µM of sample-unique forward primers and 3 µM common reverse primers (LGC Biosearch Technologies). Multimer pools (diluted 1:10,000) used for PBMC staining were also analyzed in triplicate as baselines. The PCR reaction was performed as previously decribed.[15] DNA barcode amplicons were purified using QIAquick PCR Purification Kit (QIAGEN), pooled and sequenced at PrimBio using an Ion Torrent PGM 318 chip (Life Technologies).

Data processing

Sequence data were processed using software package Barracoda (https://services.healthtech.dtu.dk/service.php?Barracoda-1.8) as previously described.[15] Briefly, barcodes were assigned to samples and peptides based on their patient-specific and peptide-specific sequences. Potential enrichment biases of PCR reactions were accounted for by unique molecular identifiers (UMIs) in each DNA barcode. For each sample, reads were normalized for mean read counts of baseline pMHC-multimer pool triplicates by trimmed means of M values. DNA barcodes with log2 fold changes of ≥2 and p values <0.001 were considered enriched. Downstream data analysis was carried out using R. To account for false-positive enrichment, DNA barcodes were discarded if average baseline reads for a barcode were <10% of the average of total baseline reads. Estimated frequencies were calculated based on the fraction of reads for a DNA barcode in relation to the frequency of sorted PE-conjugated or APC-conjugated pMHC-multimer^{+} CD8^{+} T cells.

RESULTS

Barcode-labeled pMHC-multimers were produced for MiHAs and viral antigens to detect and follow immune responses in 16 patients treated with alloSCT and DLI as outlined in figure 1.

Validation of stable pMHC-complexes

Prior to staining patient samples with pMHC-multimers, we validated whether peptides were successfully exchanged and formed stable pMHC-complexes.
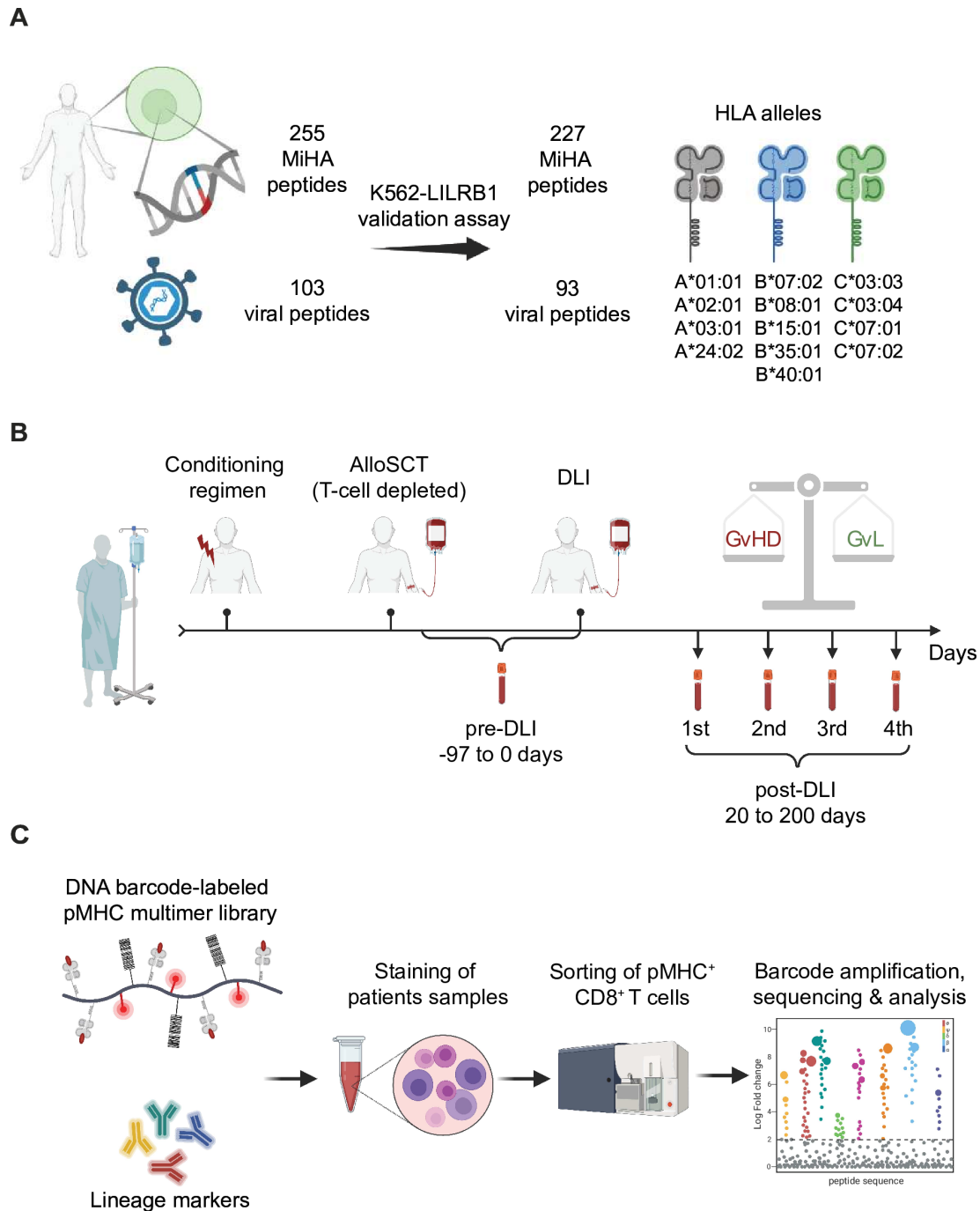
A

B

C

Figure 1 Overview of experimental setup. (A) A total of 255 MiHA peptides and 103 viral peptides were selected and evaluated for their ability to form stable pMHC-complexes with the K562-LILRB1 assay, resulting in 227 MiHA peptides and 93 viral peptides that were used for screening. (B) A cohort of 16 patients who underwent T cell-depleted alloSCT and DLI for treatment of hematological malignancies were screened. Samples before and after DLI, after which patients experienced an immune response defined by GvHD or conversion to full donor chimerism without GvHD, were analyzed. (C) Patient samples were stained with pMHC-multimer mixes and lineage markers to isolate pMHC-multimer-specific CD8+ T cells. Multimer mixes were specific for the HLA alleles as expressed by the patients. Barcodes from sorted pMHC-multimers were amplified, sequenced, and quantified to estimate peptide-specific T-cell frequencies. alloSCT, allogeneic stem cell transplantation; DLI, donor lymphocyte infusion; GvHD, graft-versus-host disease; GvL, graft-versus-leukemia; MiHA, minor histocompatibility antigen; pMHC, peptide-major histocompatibility complex.

Multimers were produced for 358 viral and MiHA peptides (figure 1A, online supplemental table 1) binding to 13 common HLA class I alleles (allele frequencies >5% in most European populations).[28]

We selected 126 autosomal MiHAs and 5 HY antigens, which were identified as T-cell targets in natural immune responses after alloSCT.[14] Additionally, 27 peptide length variants for 21 MiHAs that were

similarly recognized by T-cell clones in IFN-γ ELISA were included.[14] Furthermore, 11 polymorphic peptides that were shown to be presented by HLAs on leukemic cells or Epstein-Barr virus-transformed B cell lines by tandem mass spectrometry[29 30] and 10 published HY antigens[31] were included as well as 52 peptides for 41 allelic variants. Allelic variants were only selected if predicted to bind to the relevant HLA by NetMHCpan4.1 and mismatched in >1% of the European population,[32] or if eluted from HLA and identified by immunopeptidomics. For 12 MiHAs and allelic variants with cysteine residues, we expanded the set by 24 peptides which were cysteinylated (n=12) as potential posttranslational modification or reduced with DTT (n=12). In total, 255 polymorphic peptide variants and 103 viral antigens were included. For all polymorphic peptides, referred to as MiHAs in this study, pMHC-multimers were labeled with PE, whereas pMHC-multimers with viral epitopes were labeled with APC.

Since peptides do not always form stable pMHC-complexes by UV-mediated peptide exchange, all pMHC-multimers were validated for stability using the K562 cell line retrovirally transduced with LILRB1.[33] LILRB1 binds to parts of β2 microglobulin (β2M) and the α3 domain of the MHC heavy chain,[34] and thus only binds to stable pMHC-complexes. If peptides of interest stably bind to the fluorophore-conjugated MHC, K562-LILRB1 cells are stained by pMHC-multimers as shown for LB-APO-BEC3B-2K as example (figure 2A, left). If peptides do not stably bind to MHC, β2M dissociates from the MHC heavy chain conjugated to the fluorophore-labeled backbone, leaving K562-LILRB1 cells unstained as shown for a shorter length variant of LB-APOBEC3B-2K (figure 2A, middle).

For peptides binding to HLA-A*02:01, pMHC-multimers were produced using disulfide-stabilized HLA molecules with empty peptide-binding grooves, which provide better T-cell staining.[35] As these pMHC-multimers are stable independent of peptide binding, we adapted the K562-LILRB1 assay for HLA-A*02:01 and tested stable binding of the peptide of interest to the MHC by adding an FITC-labeled competitor peptide (FLPSDC(FITC)FPS).[26] A peptide that stably binds to MHC cannot be competed out by the FITC-labeled peptide as illustrated for HA-1 as example (figure 2B, left), whereas the FITC-labeled peptide can compete with a peptide that does not stably bind to MHC, resulting in FITC- and PE-positive K562-LILRB1 cells as displayed for the allelic variant of HA-1 (figure 2B, middle).

The K562-LILRB1 assay also allowed selection of correct peptide length variants. T-cell clones for LB-APOBEC3B-2K, LB-RPS14-1K, LB-ZNFX1-1Q and LB-ZDHHC6-1Y produced similar levels of IFN-γ upon stimulation with different peptide length variants, but for each of these MiHAs, peptides were excluded due to their failure to form stable pMHC-complexes. In total, 38 pMHC-multimers (28 MiHAs; 10 viral antigens) could not be validated as stable exogenously peptide-loaded pMHC-complexes, resulting in 227 MiHA and 93 viral peptides (figure 1).

Patient cohort

To investigate the potential of barcode-labeled pMHC-multimers to measure MiHA-specific T cells, we selected 16 transplanted patients from a cohort previously screened for MiHA identification.[14] Patients with various hematological malignances were treated with T cell-depleted alloSCT followed by pre-emptive or prophylactic DLI (table 1; Online supplemental table 2). The selected patients responded to DLI by an immune response in the form of conversion to full donor chimerism without GvHD (n=3), limited GvHD without requiring systemic immuno-suppression (n=3) or severe GvHD necessitating systemic immunosuppression (n=10). The patients received transplants from related (n=4) or unrelated (n=12) donors with a sex mismatch for 11 patient–donor pairs. From all patients, we previously successfully isolated MiHA-specific T-cell clones (online supplemental table 2).[14] Patient samples were selected before and after DLI (figure 1B). Of the 16 patients, 12 patients responded to the first DLI. The other four patients responded to a subsequent DLI (online supplemental table 2). For these patients, pre-DLI samples were selected after previous DLIs, but prior to the DLI to which the patient clinically responded. For two patients, a sample from the donor or a pretransplantation sample was analyzed as pre-DLI sample.

Detection of MiHA-specific T cells by barcoded pMHC-multimers

To measure antigen-specific T cells in patients treated with alloSCT and DLI, PE-conjugated pMHC-multimers with MiHAs and APC-conjugated pMHC-multimers with viral antigens were mixed according to the HLAs as expressed by respective patients. After incubation with PBMCs, pMHC-multimer⁺ CD8⁺ T cells for MiHAs and viral antigens were separately sorted, and DNA barcodes were amplified and sequenced (figure 1C). Sequence data were evaluated using Barracoda 1.8,[15] and enriched barcodes were defined by a ≥2 log2 fold change and p<0.001. Based on count fractions of enriched barcodes within sorted PE-conjugated or APC-conjugated pMHC-multimer⁺ CD8⁺ T cells relative to the total number of CD8⁺ T cells in the sample, frequencies of pMHC-multimer-specific CD8⁺ T cells were estimated (figure 3A). MiHAs were annotated for each patient as "mismatched" if the patient was antigen-positive (homozygous or heterozygous positive for the MiHA-encoding SNP) and the donor antigen-negative (homozygous negative for the MiHA-encoding SNP) based on SNP genotyping[14] (online supplemental table 3). MiHAs were annotated as "non-mismatched" if donors were antigen-positive and patients were antigen-negative, or if patients and donors were both either antigen-positive or antigen-negative.
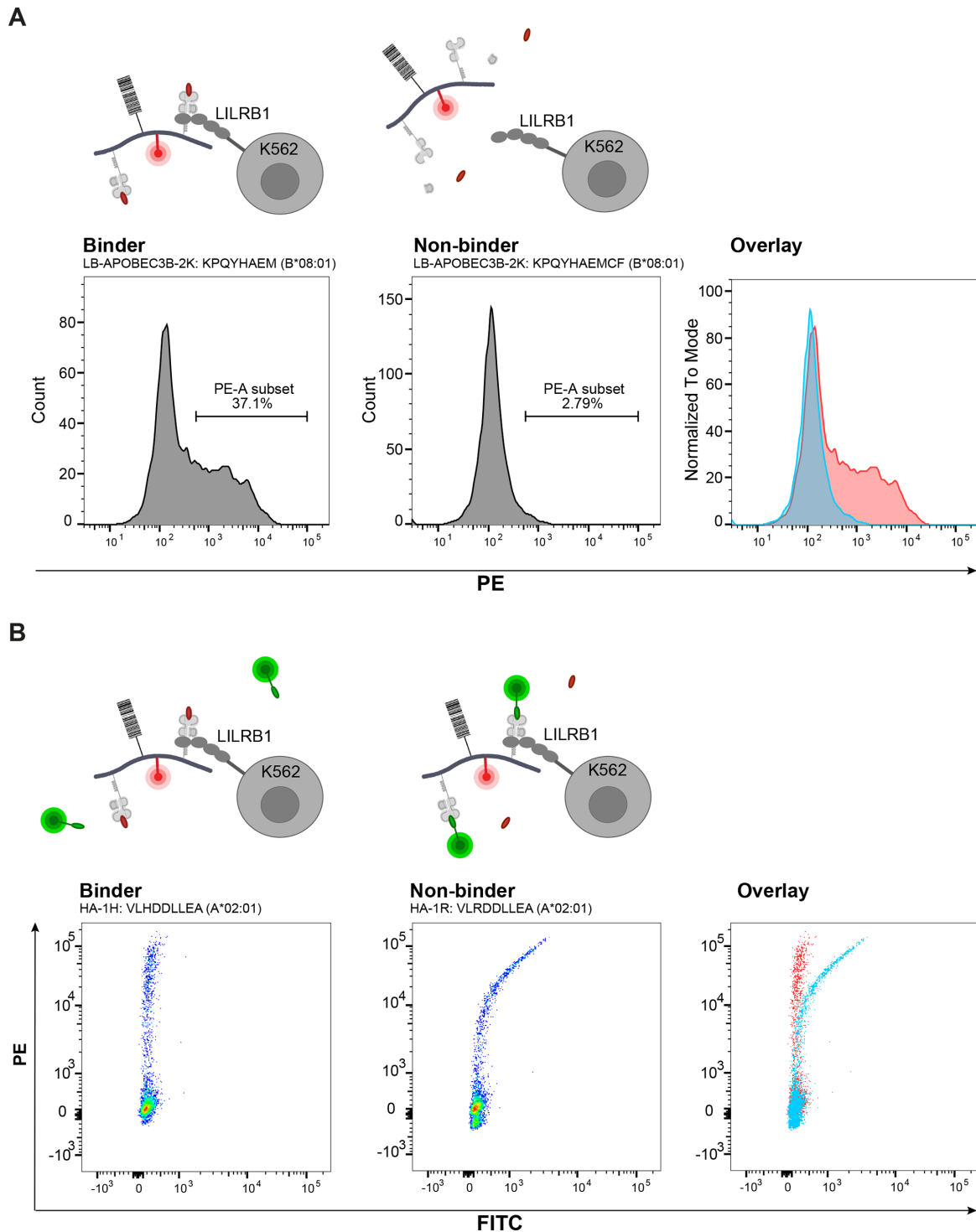
Figure 2 Validation of peptides forming stable pMHC-complexes. (A) For pMHC-multimers that were produced by UV exchange, peptides were validated for their ability to form stable pMHC-complexes using K562 cells transduced with LILRB1, which binds to β2M as well as to the α3 domain of the MHC heavy chain. On addition, stable PE-labeled pMHC-complexes result in staining of LILRB1-transduced K562 cells. As examples, two peptide length variants are shown for LB-APOBEC3B-2K. Peptide KPQYHAEM binds to HLA-B*08:01 and leads to a stable pMHC-complex (left), whereas peptide KPQYHAEMCF does not bind and leads to an unstable pMHC-complex (middle). Both examples are also overlaid (right). (B) For pMHC-multimers that were produced using stabilized HLAs (HLA-A*02:01 and A*24:02), peptides were validated for stable binding in these pMHCs by adding a FITC-labeled peptide in the K562-LILRB1 assay. If the peptide stably binds in the pMHC, it cannot be outcompeted by the FITC-labeled peptide, leading to K562-LILRB1 cells that are exclusively stained with PE-labeled pMHC-complexes (left; HA-1 (VLHDDLLEA) stably binding to HLA-A*02:01). If the peptide does not stably bind, it is outcompeted by the FITC-labeled peptide leading to K562-LILRB1 cells that are stained with both PE-labeled and FITC-labeled pMHC-complexes (middle; allelic variant HA-1R (VLRDDLLEA) not stably binding). Overlay of both examples are displayed on the right. pMHC, peptide-major histocompatibility complex; PE, phycoerythrin.

Table 1 Patient cohort screened for MiHA-specific T cells by DNA barcoded pMHC-multimers

		Total	No GvHD	Limited GvHD	Severe GvHD
	Patients	16	3	3	10
Sex (donor→patient)	f→f	4	1	0	3
	f→m	11	1	3	7
	m→m	1	1	0	0
Relation to donor	Unrelated donor	12	2	3	7
	Related donor	4	1	0	3
HLA matching	10/10	1	0	1	0
	10/12	3	1	0	2
	11/12	4	0	1	3
	12/12	8	2	1	5
Disease	AML	8	1	2	5
	CLL	1	1	0	0
	CML	2	1	0	1
	MDS	2	0	1	1
	MM	3	0	0	3
Donor/recipient HLA type	A*01:01	10	2	1	7
	A*02:01	9	2	2	5
	A*03:01	5	1	0	4
	A*24:02	2	0	2	0
	B*07:02	10	2	1	7
	B*08:01	10	1	1	8
	B*15:01	2	1	1	0
	B*40:01	1	0	1	0
	C*03:03	2	1	1	0
	C*03:04	1	0	1	0
	C*07:01	12	2	1	9
	C*07:02	10	2	1	7

AML, acute myeloid leukemia; CLL, chronic lymphocytic leukemia; CML, chronic myeloid leukemia; GvHD, graft-versus-host disease; MDS, myelodysplastic syndrome; MiHA, minor histocompatibility antigens; MM, multiple myeloma; pMHC, peptide-major histocompatibility complex.

To assess potential background staining of MiHA-specific pMHC-multimers, each patient-specific pMHC-multimer mix was tested on PBMCs from pooled healthy individuals (n=3) containing at least one donor expressing the HLA of interest. In total, 10 pMHC-multimers showed enrichment in healthy donor pools (online supplemental figure 1). Four of these pMHC-multimers were also each enriched in 4–7 patients who were not mismatched for these antigens (online supplemental table 4), and therefore, excluded from analysis. One of these four pMHC-multimers was LB-ZNF419-2G. For this MiHA, a high T-cell frequency of 4.8% was detected in patient #10605 from whom we previously isolated T-cell clones against LB-ZNF419-2G, indicating that exclusion of this pMHC-multimer not only eliminated non-specific, but also true T-cell responses.

To avoid overestimation of T-cell frequencies, we grouped MiHAs and chemically modified or length variants that may potentially bind to the same T cells. For each sample, the peptide with the highest measured T-cell frequency within each group was selected for further analysis (online supplemental table 1). We further noticed in 6 samples that T cells were detected for MiHAs as well as their allelic variants (online supplemental figure 2). If allelic variants are not naturally presented on the cell surface due to intracellular cleavage or insufficient binding affinity to HLA, T cells specific for allelic variants may have escaped negative selection. These T cells may not be able to discriminate between MiHAs and allelic variants when artificially presented in pMHCs.[36] Therefore, when T-cell frequencies were detected for both MiHAs and allelic variants in one sample, the peptide with the highest T-cell frequency was selected irrespective of SNP genotyping for the respective patient–donor pair.

In total, 88 distinct T-cell responses were detected against 49 different MiHAs. For these 49 MiHAs, responses were
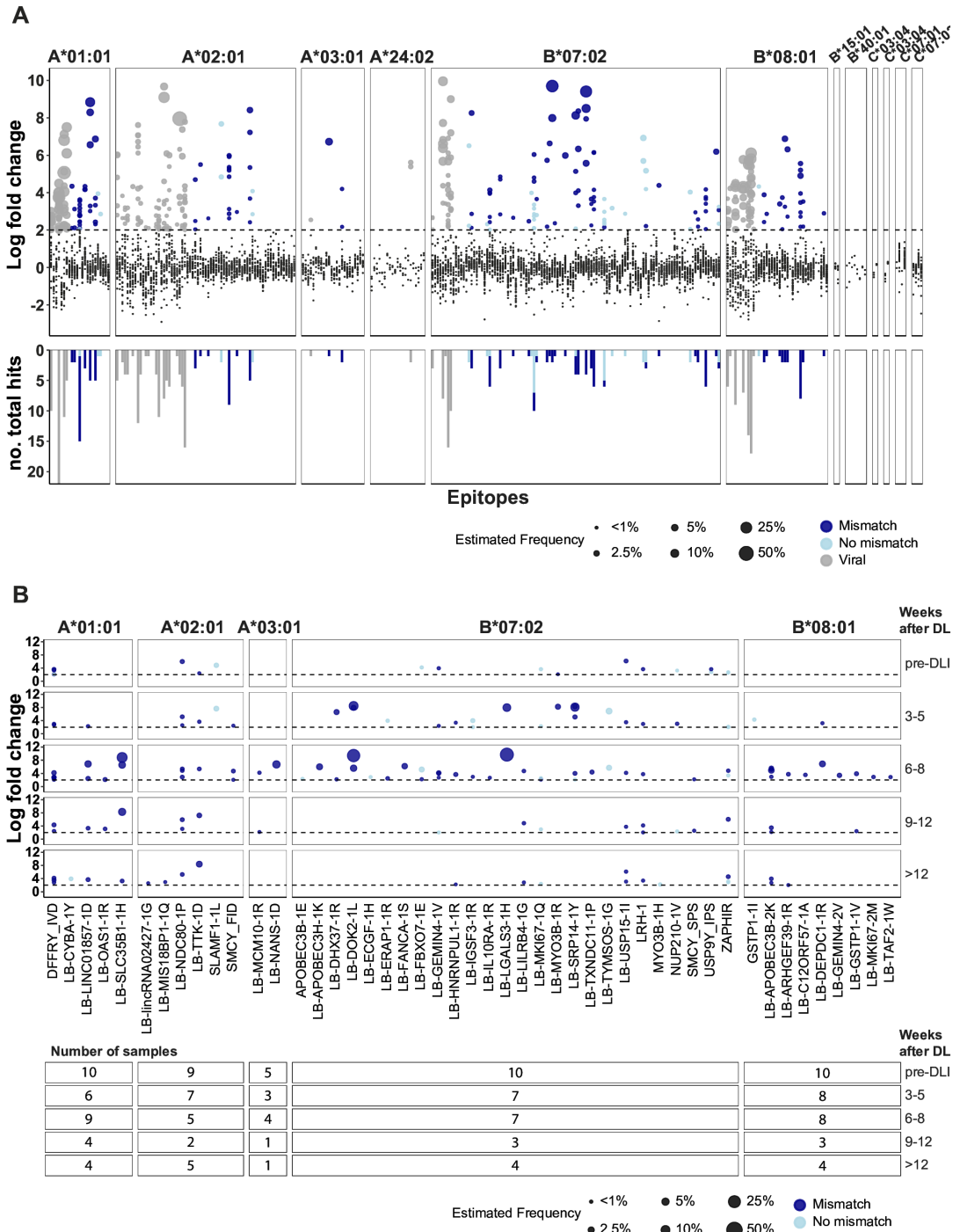
Figure 3 Barcode-labeled pMHC-multimer detection of antigen-specific T cells in patients treated with alloSCT and DLI. (A) Overview of all DNA barcode measurements for samples from patients treated with alloSCT and DLI. Enriched barcodes were defined by a ≥2 log2 fold change and p<0.001 calculated using the Barracoda 1.8 pipeline.[15] Enriched barcodes in the upper panel are colored for MiHAs that are mismatched (dark blue) or non-mismatched (light blue) in the respective patient-donor pairs, or for viral peptides (gray). Black data points with a log2 fold change <2 represent barcodes that were not significantly enriched (upper panel). Dot sizes represent estimated frequencies of the antigen-specific CD8^{+} T cells in the respective sample. The lower panel indicates the number of samples per barcode for which statistically significant enrichment was measured. (B) Enriched barcodes for MiHAs in alloSCT patients during treatment with DLI are shown for indicated time periods. All indicated antigens are validated MiHAs except for SLAMF1-1L, APOBEC3B-1E, MYO3B-1H, NUP210-1V, and GSTP1-1I, which are allelic variants of MiHAs. The table displays the number of samples included for indicated time periods. Within each time period, measurements for the sample with the highest total estimated T-cell frequency for MiHAs is shown for each patient. Multimers containing peptide length variants for MiHAs and allelic variants that may potentially bind to the same T cells were grouped, and the pMHC-multimer with the highest fold change within each group was selected per sample. alloSCT, allogeneic stem cell transplantation; DLI, donor lymphocyte infusion; MiHAs, minor histocompatibility antigens; pMHC, peptide-major histocompatibility complex.

directed against 31 antigens only in patients mismatched for these MiHAs, 10 antigens in patients mismatched as well as patients not mismatched for these antigens, and 8 antigens for which responses were detected only in patients who were not mismatched. Of the 88 distinct T-cell responses, 64 (72.7%) responses were detected in patients mismatched for these antigens (figure 3B, online supplemental table 5). Of the 24 (27.3%) responses against non-mismatched MiHAs, 11 responses were found in antigen-negative patients transplanted with antigen-negative donors. Detection of these responses may be explained by induction of MiHA-specific T cells in donors as a result of prior pregnancies[37 38] or blood transfusions. Of the 13 responses detected in patients transplanted with antigen-positive donors, three T-cell responses were found in patients who were positive for the allelic variant, whereas the donor was homozygous positive for the MiHA. The detected immune responses may have been induced against the allelic variant, for which patients were mismatched instead of the MiHA, but falsely detected as specific for the MiHA, if the allelic variant was not included in this study and T cells were also able to bind to the MiHA when artificially presented by pMHC-multimers. Of the three T-cell responses that may potentially be directed against allelic variants instead of MiHAs, two allelic variants were not included in the peptide selection (MKI67-1R, ECGF-1R), and one allelic variant was excluded because of potential non-specific binding (LB-ZNF419-2G, allelic variant of ZAPHIR). Therefore, detection of T cells against LB-MKI67-1Q, LB-ECGF1-1H and ZAPHIR in patients who were not mismatched for these antigens may potentially be caused by T-cell responses directed against the allelic variants MKI67-1R, ECGF-1R and LB-ZNF419-2G, for which the patients were mismatched. Finally, for the other 10 responses against non-mismatched MiHAs, T cells may have been detected due to low affinity or non-specific pMHC-multimer binding.

To evaluate whether T-cell responses against non-mismatched MiHAs are true responses or caused by non-specific binding of barcoded pMHC-multimers, we produced high-quality conventional fluorescent pMHC-tetramers assembled from pMHC-monomers folded with peptides of interest for 13 immune responses that were detected in patients #8905 and #7956 by barcoded pMHC-multimers. Of the 13 immune responses, 9 responses against mismatched MiHAs were confirmed with conventional pMHC-tetramer staining (online supplemental table 6). Also the high T-cell frequency against the non-mismatched MiHA LB-TYMSOS-1G, for which patient #7956 and the corresponding donor were both antigen-negative, was confirmed by conventional pMHC-tetramer staining. However, the pMHC-tetramer against LB-IGSF3-1R, which was non-mismatched in #7956, showed background staining on healthy donor PBMCs, suggesting that also the responses detected for this MiHA by conventional pMHC-tetramer and barcoded pMHC-multimer staining were caused by non-specific binding. The low T-cell frequencies against LB-FBXO7-1E, which was mismatched in patient #8905 and non-mismatched in patient #7956, could not be confirmed and may have been caused by non-specific binding of barcoded pMHC-multimers.

T-cell frequencies against MiHAs

We reasoned that clinically relevant T cells expand after DLI coinciding with conversion to full donor chimerism or development of GvHD. Moreover, clinically relevant T cells are expected to remain detectable longitudinally in multiple samples after DLI. Of all 153 measurements for 88 distinct T-cell responses, 121 measurements were directed against mismatched MiHAs and 32 measurements against non-mismatched MiHAs. Out of 121 T-cell measurements targeting mismatched MiHAs, the majority were detected after DLI (111 of 121; 91.7%). Of these 111 measurements, 59 (53.2%) were detected with T-cell frequencies between 0.1%–1% and 21 measurements (18.9%) with frequencies above 1% of CD8$^+$ T cells (online supplemental table 5). For 32 T-cell measurements against non-mismatched MiHAs, 24 (75.0%) responses were detected after DLI. Of these 24 T-cell responses, only 6 (25.0%) and 4 (16.7%) responses were measured with frequencies between 0.1%–1% and above 1% of CD8$^+$ T cells, respectively. In 11 patients for whom more than one post-DLI sample was screened, T cells against 29 (63.3%) of the 49 mismatched MiHAs that were targeted and 45 (45.9%) of 98 viral antigens were measured in more than one post-DLI sample of the same patient (figure 4A). In contrast, only 3 (21.4%) out of 14 T-cell measurements for non-mismatched MiHAs were detected in multiple patient samples. For the majority of patients, total T-cell frequencies for mismatched MiHAs showed expansion after DLI, peaking at frequencies above 1% around 6–8 weeks after DLI when patients typically experienced a clinical response (figure 4B). This was in contrast to non-mismatched MiHAs, for which the majority of patients had total frequencies below 0.1% after DLI. These frequencies showed a small increase between 3 and 5 weeks after DLI, but only low or undetectable levels at the onset of clinical responses. Also for viral antigens, no increase in T-cell frequencies was observed at the onset of clinical responses (figure 4B, online supplemental figure 4). Thus, T-cell responses typically peaked at 6–8 weeks after DLI and were directed against mismatched MiHAs, while T-cell responses against non-mismatched MiHAs were not relevant for development of clinical responses after alloSCT.

Composition of immune responses against MiHAs

We next analyzed the composition of immune responses after DLI in patients with no, limited or severe GvHD with respect to measured T-cell
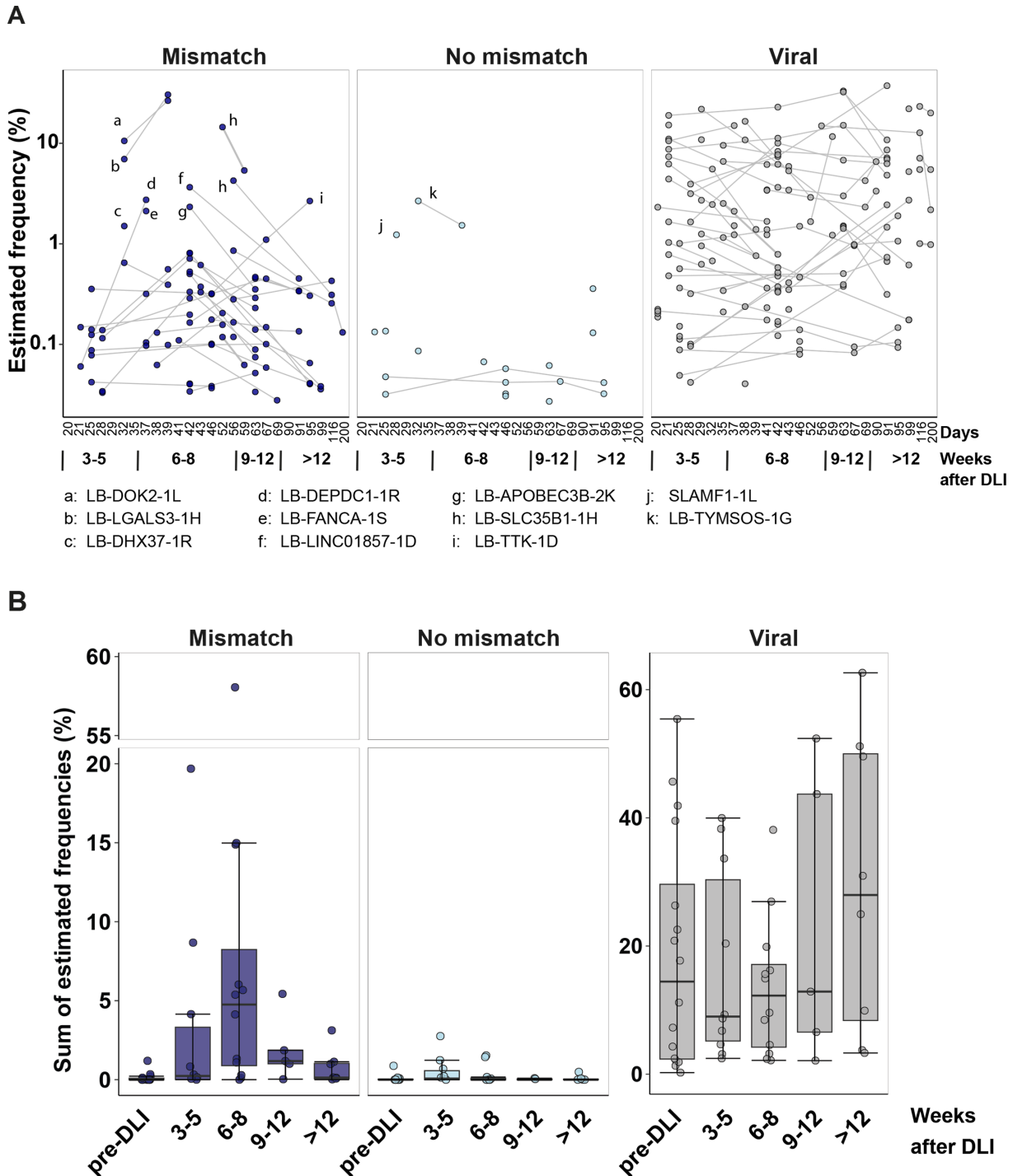
Figure 4 Frequencies of MiHA-specific T cells in patient samples. (A) Indicated are estimated T-cell frequencies by pMHC-multimers with MiHAs that are mismatched (dark blue) or not mismatched (light blue) or pMHC-multimers with viral peptides (gray) in alloSCT patients after treatment with DLI. Data are shown for 11 patients with multiple samples after DLI screened by pMHC-multimers. In contrast to non-mismatched MiHAs, enriched barcodes for mismatched MiHAs and viral antigens were often detected in multiple samples after DLI indicated by connecting lines. (B) The sum of estimated T-cell frequencies is shown for all pMHC-multimers with mismatched or non-mismatched MiHAs or pMHC-multimers with viral peptides for each time period. Two patients were excluded as barcode sequence data were missing for post-DLI samples. alloSCT, allogeneic stem cell transplantation; DLI, donor lymphocyte infusion; MiHAs, minor histocompatibility antigens; pMHC, peptide-major histocompatibility complex.

frequencies and type of MiHAs. High total MiHA-specific T-cell frequencies between 1.3% and 59.6% of CD8$^+$ T cells were observed in all 10 patients

with severe GvHD and 2 patients with limited GvHD (figure 5A, online supplemental table 5). Of three patients without GvHD, patient #4739 also had total
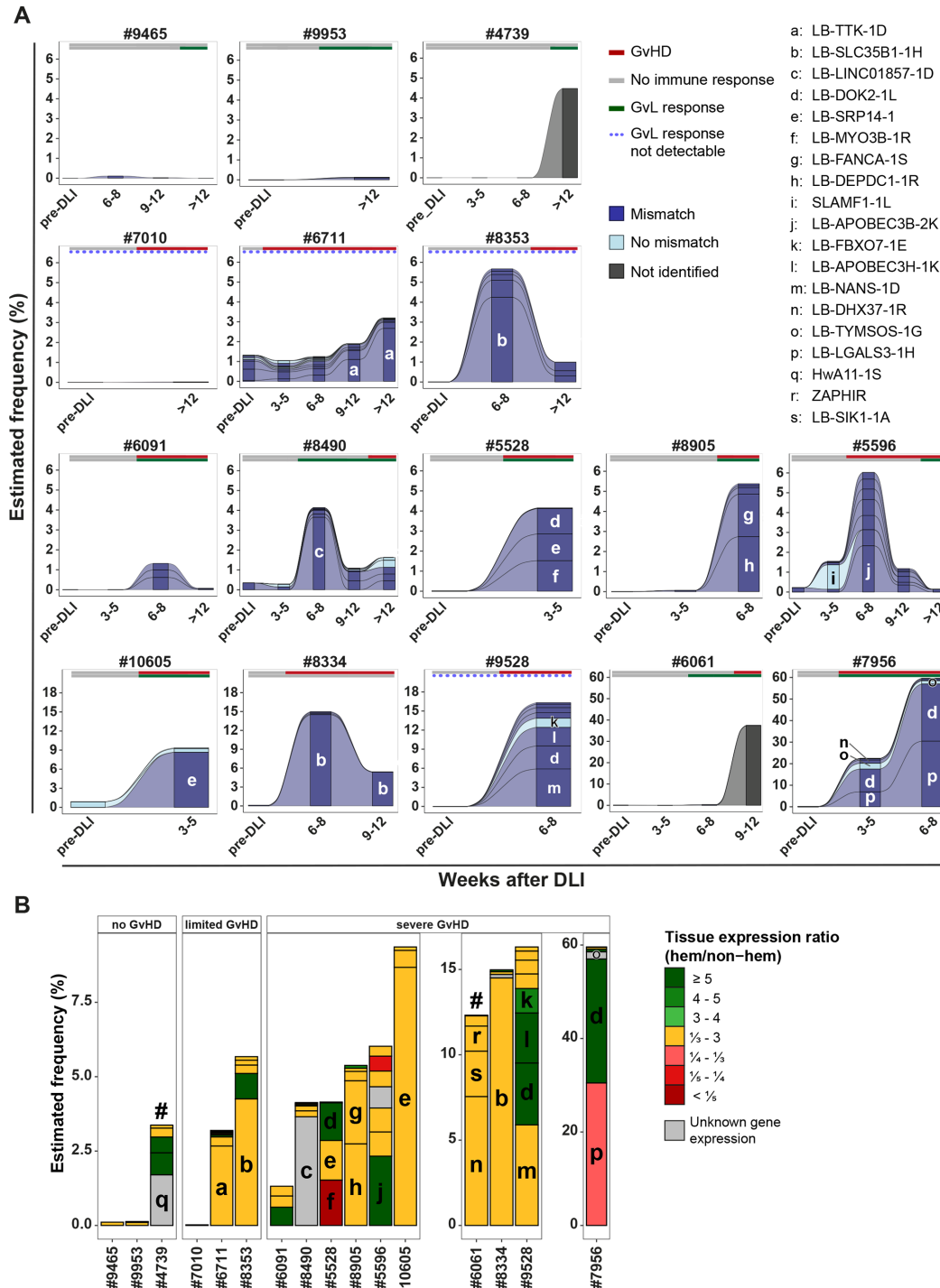
Figure 5 Kinetics of MiHA-specific T cells in 16 patients who responded to DLI after HLA-matched alloSCT. (A) Estimated frequencies of MiHA-specific T cells by pMHC-multimer staining are shown for 16 patients who responded to DLI after HLA-matched alloSCT. Of the 16 patients, 3 patients responded to DLI without GvHD (patients #9465, #9953, #4739), 3 patients developed limited GvHD (patients #7010, #6711, #8353) and 10 patients had severe GvHD (#6091, #8490, #5528, #8905, #5596, #10605, #8334, #9528, #6061, #7956) after DLI. Each stack represents the estimated T-cell frequency for a MiHA that is mismatched (dark blue) or not mismatched (light blue) in the respective patient. For two samples (gray), frequencies of pMHC-multimer⁺ T cells measured during FACS sorting are displayed, but barcode sequence data were not determined due to PCR failure. Letters indicate MiHAs for which estimated T-cell frequencies of ≥1% of CD8⁺ T cells were detected. (B) Tissue expression of MiHAs targeted by T cells for the sample with the highest measured T-cell frequencies of each patient. Hashtags indicate two samples in which T-cell frequencies were measured by conventional pMHC-tetramer staining as barcode sequence data were missing. Colors indicate relative expression of the MiHA encoding gene in hematopoietic compared with non-hematopoietic cells using single cell RNA-Seq data of the Human Protein Atlas. alloSCT, allogeneic stem cell transplantation; DLI, donor lymphocyte infusion; GvHD, graft-versus-host disease; GvL, graft-versus-leukemia; MiHAs, minor histocompatibility antigens; pMHC, peptide-major histocompatibility complex.

frequencies above 1%, showing that high frequencies of MiHA-specific T cells do not necessarily induce GvHD.

Patients typically showed a peak in T-cell expansion around 6–8 weeks after DLI except for three patients. For patients #9953 and #4739, high MiHA-specific T-cell frequencies were detected on days 98 (14 weeks) and 139 (~20 weeks) after DLI, respectively, correlating with late conversion to full donor chimerism (online supplemental figure 5). Patient #6711, who had already converted to full donor chimerism after a first low-dose DLI, showed increased T-cell frequencies after a second high-dose DLI, which continued to rise until the last analyzed sample on day 96 (~14 weeks) when the patient received topical immunosuppression for limited GvHD (online supplemental figure 5).

To determine the potential contribution of MiHAs to development of GvL or GvHD, expression of the antigen-encoding genes was retrieved from single cell RNA-seq data of the Human Protein Atlas. As previously described,[14] gene expression was compared in hematopoietic versus non-hematopoietic single cell clusters of tissues typically affected by GvHD, and a ratio was calculated based on maximum expression values in the two groups. For two patients #4739 and #6061, the type of MiHAs targeted after DLI could not be determined by barcode-labeled pMHC-multimers due to PCR failure. We, therefore, performed conventional pMHC-tetramer staining of a BMMC sample taken on the same day from patient #4739 and a PBMC sample obtained 4 days after the previously analyzed sample from patient #6061. Tetramer staining was performed for all MiHAs for which we had previously isolated T-cell clones from these patients (online supplemental table 2).

In all patient groups, T cells against MiHAs with broad as well as hematopoietic expression were found. In five patients with GvHD, immune responses were largely dominated by T cells against single MiHAs with broad (LB-TTK-1D in patient #6711; LB-SL-C35B1-1H in patients #8353 and #8334; LB-SRP14-1 in patient #10605) or unknown (LB-LINC01857-1D in patient #8490) gene expression (figure 5B). In patient #6711, T-cell frequencies against LB-TTK-1D gradually increased after the second DLI until diagnosis of GvHD, while T-cell frequencies against other MiHAs did not change or decreased (online supplemental figure 5). In other GvHD patients, high T-cell frequencies were found against multiple MiHAs with varying tissue distribution. Patient #7956 developed severe grade 4 GvHD of the gastrointestinal tract and grade 3 GvHD of the skin (online supplemental table 2, online supplemental figure 5). In this patient, high T-cell frequencies were directed against the hematopoietic-restricted LB-DOK2-1L (26.5%) as well as LB-LGALS3-1H (30.5%), which is encoded by *LGALS3*, a gene highly expressed particularly in colon epithelial cells.

In conclusion, our data demonstrate that barcode-labeled pMHC-multimers can be used to detect and monitor MiHA-specific T cells in patients who responded to DLI after HLA-matched alloSCT. Using this technology, we detected T cells against a variety of MiHAs with different tissue distribution profiles at higher frequencies in patients with GvHD, indicating that these may be particularly relevant in immune responses after alloSCT.

DISCUSSION

Measuring T-cell frequencies against MiHAs is challenging due to the large number of potential targets and limited sample availability. Here, we screened 16 transplanted patients and showed that barcoded pMHC-multimer screening is a feasible method to detect and monitor CD8$^+$ T cells against a large set of MiHAs. Variable T-cell frequencies up to 30.5% of CD8$^+$ T cells against MiHAs with different tissue distribution profiles were measured, and high T-cell frequencies were typically observed 6–8 weeks after DLI at onset of GvHD.

Various studies have previously measured SNP mismatches between patients and donors and attempted to associate total SNP mismatches or selected SNP mismatches for predicted or identified MiHAs with clinical outcome after HLA-matched alloSCT with no or limited success.[8 9 11 39] In these studies, SNP mismatches or predicted MiHAs were considered to equally contribute to clinical outcome, whereas clinical outcome is more likely to be determined by immunodominant MiHAs that are targeted with high T-cell frequencies, and to a lesser extent by MiHAs targeted with no or low T-cell frequencies. Here, we showed that the landscape of MiHAs is targeted by a vast range of T-cell frequencies from barely detectable to 30.5% of CD8$^+$ T cells. The existence of immunodominance illustrates the difficulty to associate SNP mismatches or predicted MiHAs with GvL and GvHD after HLA-matched alloSCT, and emphasizes the need to determine immunodominant MiHAs for accurate detection and potential prediction of GvL and GvHD after alloSCT. Whether T-cell frequencies measured in blood or bone marrow reflect the state of GvHD-affected organs is disputed. Using T-cell receptor sequencing, studies showed overlap, but also vastly different compositions of the T-cell receptor repertoire in GvHD-affected tissues and blood.[40 41] However, Sacirbegovic *et al*[42] showed in mouse studies, an overlap of TCR repertoires due to influx of alloreactive T cells from blood to tissues in early GvHD and subsequent diversification in late GvHD due to local maintenance of tissue-resident progenitor-like T cells. We often observed that T-cell frequencies peak at the onset of clinically diagnosed GvHD, suggesting that MiHA-specific T cells measured

in peripheral blood during induction of the immune response may provide a snapshot of the MiHA repertoire that will locally stimulate tissue-infiltrating T cells in the upcoming immune response.

Since only mismatched MiHAs are foreign to the transplanted donor-derived immune system, measuring T cells against non-mismatched MiHAs was unexpected, in particular since all MiHA-specific T-cell clones previously isolated from these patients were only directed against mismatched MiHAs.[14] T cells for non-mismatched MiHAs were often detected with low frequencies, were present already before DLI and did not expand after DLI. This indicates that T cells against non-mismatched MiHAs are not relevant for development of GvL and GvHD after DLI. All T-cell frequencies above 1% of CD8$^+$ T cells against non-mismatched MiHAs were observed in antigen-negative patients transplanted with antigen-negative donors. Since most stem cell donors in our cohort were female, donors may have been sensitized on antigen exposure during prior pregnancies.[37 38] T-cell responses against non-mismatched MiHAs that were detected in multiple samples of the same patient were either found in these antigen-negative patients transplanted with antigen-negative donors, or in antigen-negative patients transplanted with antigen-positive donors who were mismatched for the allelic variant that may have been the actual target for the detected T cells. However, we also measured T-cell responses against non-mismatched MiHAs in patients transplanted with antigen-positive donors that could not be specific for allelic variants. These T-cell frequencies may be caused by virus-specific T cells or T cells for other pathogens that are cross-reactive[43] or by non-specific binding of barcoded pMHC-multimers. For two MiHAs in patient #7956, low T-cell frequencies were probably the result of non-specific binding since the responses could not be confirmed by conventional fluorescent pMHC-tetramers. Alternatively, since not all T cells stained with pMHC-multimers are functional,[44 45] T cells may also cross-react against MiHAs with an avidity that is too low to target the antigen, but sufficient to bind to pMHCs. Therefore, to avoid overestimation of irrelevant measurements, especially T-cell responses at low frequencies need to be carefully evaluated.

Results from this pilot study support our previous findings that T-cell frequencies in patients with GvHD are higher than in patients without GvHD.[46] Since our patient cohort is small and selected, conclusions about association of MiHAs with clinical outcome after HLA-matched alloSCT cannot be drawn, and require screening of large patient cohorts to investigate whether and which MiHAs allow prediction of GvL and GvHD after alloSCT. T-cell responses for GvHD-associated MiHAs are probably high during active GvHD, but low or undetectable in absence of GvHD, whereas T-cell responses for GvL-associated MiHAs may also be present at high frequencies in patients without GvHD, as reported for HA-1 and HA-2.[47] Further research needs to be done to determine whether MiHAs can be associated with GvL or GvHD, and which T-cell frequencies are required for an effective clinical response. Furthermore, it needs to be evaluated whether a hierarchy in immunodominance exists among MiHAs similar as described for viral epitopes,[48] which may result in MiHAs only being immunodominant in patients if other more immunodominant MiHAs are absent, and how the landscape of targeted MiHAs is influenced by an inflammatory environment, which stimulates presentation and recognition of MiHAs.

By monitoring 16 patients who responded to DLI after HLA-matched T-cell depleted alloSCT with barcoded pMHC-multimers, we confirmed previous findings that peak T-cell frequencies against MiHAs are typically induced 6–8 weeks after DLI.[46 47] Currently, patients are increasingly treated with post-transplantation cyclophosphamide (PTCy) shortly after alloSCT as GvHD prophylaxis.[49 50] Since patients often develop effective GvL responses, MiHA-specific T-cell responses are also expected to be induced and target tumor cells after HLA-matched PTCy-alloSCT. Barcoded pMHC-multimers may be used to investigate the strength, breadth and kinetics of MiHA-specific T-cell responses, which is particularly relevant in patients treated with PTCy-alloSCT, since most patients do not develop GvHD, and therefore, lack clinical signs for development of an effective immune response after alloSCT.

In conclusion, we here evaluated and established barcode-labeled pMHC-multimer screening as a feasible method to detect and follow MiHA-specific T cells in large patient cohorts, which is crucial to elucidate how GvL and GvHD after alloSCT are orchestrated and how MiHAs can be used to improve clinical outcome after alloSCT.

ORCID iDs
Kyra J Fuchs http://orcid.org/0000-0002-4704-8218
Eva A S Koster http://orcid.org/0000-0002-8446-5133
Ferenc Scheeren http://orcid.org/0000-0002-8304-9023
Mirjam H M Heemskerk http://orcid.org/0000-0001-6320-9133
Sine R Hadrup http://orcid.org/0000-0002-5937-4344

REFERENCES

1. Biernacki MA, Sheth VS, Bleakley M. T cell optimization for graft-versus-leukemia responses. *JCI Insight* 2020;5:e134939.
2. van der Zouwen B, Koster EAS, von dem Borne PA, *et al*. Feasibility, safety, and efficacy of early prophylactic donor lymphocyte infusion after T cell-depleted allogeneic stem cell transplantation in acute leukemia patients. *Ann Hematol* 2023;102:1203–13.
3. Schmid C, Labopin M, Schaap N, *et al*. Long-term results and GvHD after prophylactic and preemptive donor lymphocyte infusion after allogeneic stem cell transplantation for acute leukemia. *Bone Marrow Transplant* 2022;57:215–23.
4. Spierings E. Minor histocompatibility antigens: past, present, and future. *Tissue Antigens* 2014;84:374–60.
5. Griffioen M, van Bergen CAM, Falkenburg JHF. Autosomal Minor Histocompatibility Antigens: How Genetic Variants Create Diversity in Immune Targets. *Front Immunol* 2016;7:100.
6. Hobo W, Broen K, van der Velden W, *et al*. Association of disparities in known minor histocompatibility antigens with relapse-free survival and graft-versus-host disease after allogeneic stem cell transplantation. *Biol Blood Marrow Transplant* 2013;19:274–82.
7. Story CM, Wang T, Bhatt VR, *et al*. Genetics of HLA Peptide Presentation and Impact on Outcomes in HLA-Matched Allogeneic Hematopoietic Cell Transplantation. *Transplant Cell Ther* 2021;27:591–9.
8. Martin PJ, Levine DM, Storer BE, *et al*. Genome-wide minor histocompatibility matching as related to the risk of graft-versus-host disease. *Blood* 2017;129:791–8.
9. Martin PJ, Levine DM, Storer BE, *et al*. A Model of Minor Histocompatibility Antigens in Allogeneic Hematopoietic Cell Transplantation. *Front Immunol* 2021;12:782152.
10. Lansford JL, Dharmasiri U, Chai S, *et al*. Computational modeling and confirmation of leukemia-associated minor histocompatibility antigens. *Blood Adv* 2018;2:2052–62.
11. Jadi O, Tang H, Olsen K, *et al*. Associations of minor histocompatibility antigens with outcomes following allogeneic hematopoietic cell transplantation. *Am J Hematol* 2023;98:940–50.
12. Mutis T, Xagara A, Spaapen RM. The Connection Between Minor H Antigens and Neoantigens and the Missing Link in Their Prediction. *Front Immunol* 2020;11:1162.
13. Hombrink P, Hassan C, Kester MGD, *et al*. Identification of Biological Relevant Minor Histocompatibility Antigens within the B-lymphocyte-Derived HLA-Ligandome Using a Reverse Immunology Approach. *Clin Cancer Res* 2015;21:2177–86.
14. Fuchs KJ, van de Meent M, Honders MW, *et al*. Expanding the repertoire reveals recurrent, cryptic, and hematopoietic HLA class I minor histocompatibility antigens. *Blood* 2024;143:1856–72.
15. Bentzen AK, Marquard AM, Lyngaa R, *et al*. Large-scale detection of antigen-specific T cells using peptide-MHC-I multimers labeled with DNA barcodes. *Nat Biotechnol* 2016;34:1037–45.
16. Kristensen NP, Heeke C, Tvingsholm SA, *et al*. Neoantigen-reactive CD8+ T cells affect clinical outcome of adoptive cell therapy with tumor-infiltrating lymphocytes in melanoma. *J Clin Invest* 2022;132:e150535.
17. Toebes M, Coccoris M, Bins A, *et al*. Design and use of conditional MHC class I ligands. *Nat Med* 2006;12:246–51.
18. Frøsig TM, Yap J, Seremet T, *et al*. Design and validation of conditional ligands for HLA-B*08:01, HLA-B*15:01, HLA-B*35:01, and HLA-B*44:05. *Cytometry A* 2015;87:967–75.
19. Rodenko B, Toebes M, Hadrup SR, *et al*. Generation of peptide-MHC class I complexes through UV-mediated ligand exchange. *Nat Protoc* 2006;1:1120–32.
20. Hadrup SR, Bakker AH, Shu CJ, *et al*. Parallel detection of antigen-specific T-cell responses by multidimensional encoding of MHC multimers. *Nat Methods* 2009;6:520–6.
21. Göransson M. Decoding peptide-MHC recognition to unravel t cell involvement in type 1 diabetes and allogeneic hematopoietic stem cell transplantation [doctoral dissertation]. DTU Health Technology; 2023.
22. Burrows SR, Kienzle N, Winterhalter A, *et al*. Peptide-MHC Class I Tetrameric Complexes Display Exquisite Ligand Specificity. *J Immunol* 2000;165:6229–34.
23. Saini SK, Abualrous ET, Tigan A-S, *et al*. Not all empty MHC class I molecules are molten globules: tryptophan fluorescence reveals a two-step mechanism of thermal denaturation. *Mol Immunol* 2013;54:386–96.
24. Xu Q, Schlabach MR, Hannon GJ, *et al*. Design of 240,000 orthogonal 25mer DNA barcode probes. *Proc Natl Acad Sci U S A* 2009;106:2289–94.
25. Kivioja T, Vähärautio A, Karlsson K, *et al*. Counting absolute numbers of molecules using unique molecular identifiers. *Nat Methods* 2012;9:72–4.
26. Ottenhoff THM, Geluk A, Toebes M, *et al*. A sensitive fluorometric assay for quantitatively measuring specific peptide binding to HLA class I and class II molecules. *J Immunol Methods* 1997;200:89–97.
27. Lissina A, Ladell K, Skowera A, *et al*. Protein kinase inhibitors substantially improve the physical detection of T-cells with peptide-MHC tetramers. *J Immunol Methods* 2009;340:11–24.
28. Gonzalez-Galarza FF, McCabe A, Santos EJMD, *et al*. Allele frequency net database (AFND) 2020 update: gold-standard data classification, open access genotype data and new query tools. *Nucleic Acids Res* 2020;48:D783–8.
29. van Amerongen RA, Hagedoorn RS, Remst DFG, *et al*. WT1-specific TCRs directed against newly identified peptides install antitumor reactivity against acute myeloid leukemia and ovarian carcinoma. *J Immunother Cancer* 2022;10:e004409.
30. de Rooij MAJ, Remst DFG, van der Steen DM, *et al*. A library of cancer testis specific T cell receptors for T cell receptor gene therapy. *Mol Ther Oncolytics* 2023;28:1–14.
31. Ofran Y, Kim HT, Brusic V, *et al*. Diverse patterns of T-cell response against multiple newly identified human Y chromosome-encoded minor histocompatibility epitopes. *Clin Cancer Res* 2010;16:1642–51.
32. Sherry ST, Ward MH, Kholodov M, *et al*. dbSNP: the NCBI database of genetic variation. *Nucleic Acids Res* 2001;29:308–11.
33. Ruibal P, Franken KLMC, van Meijgaarden KE, *et al*. Identification of HLA-E Binding *Mycobacterium tuberculosis*-Derived Epitopes through Improved Prediction Models. *J Immunol* 2022;209:1555–65.
34. Willcox BE, Thomas LM, Bjorkman PJ. Crystal structure of HLA-A2 bound to LIR-1, a host and viral major histocompatibility complex receptor. *Nat Immunol* 2003;4:913–9.
35. Saini SK, Tamhane T, Anjanappa R, *et al*. Empty peptide-receptive MHC class I molecules for efficient detection of antigen-specific T cells. *Sci Immunol* 2019;4:eaau9039.
36. Pierce RA, Field ED, Mutis T, *et al*. The HA-2 minor histocompatibility antigen is derived from a diallelic gene encoding a novel human class I myosin protein. *J Immunol* 2001;167:3223–30.
37. Christiansen OB, Steffensen R, Nielsen HS. Anti-HY responses in pregnancy disorders. *Am J Reprod Immunol* 2011;66 Suppl 1:93–100.
38. Verdijk RM, Kloosterman A, Pool J, *et al*. Pregnancy induces minor histocompatibility antigen-specific cytotoxic T cells: implications for stem cell transplantation and immunotherapy. *Blood* 2004;103:1961–4.
39. Nie D, Zhang J, Liu L, *et al*. Targeted minor histocompatibility antigen typing to estimate graft-versus-host disease after allogeneic haematopoietic stem cell transplantation. *Bone Marrow Transplant* 2021;56:3024–8.
40. Koyama D, Murata M, Hanajiri R, *et al*. Quantitative Assessment of T Cell Clonotypes in Human Acute Graft-versus-Host Disease Tissues. *Biol Blood Marrow Transplant* 2019;25:417–23.
41. DeWolf S, Elhanati Y, Nichols K, *et al*. Tissue-specific features of the T cell repertoire after allogeneic hematopoietic cell transplantation in human and mouse. *Sci Transl Med* 2023;15:eabq0476.

42 Sacirbegovic F, Günther M, Greco A, *et al*. Graft-versus-host disease is locally maintained in target tissues by resident progenitor-like T cells. *Immunity* 2023;56:369–85.

43 Jiang N, Malone M, Chizari S. Antigen-specific and cross-reactive T cells in protection and disease. *Immunol Rev* 2023;316:120–35.

44 Roex MCJ, Hageman L, Veld SAJ, *et al*. A minority of T cells recognizing tumor-associated antigens presented in self-HLA can provoke antitumor reactivity. *Blood* 2020;136:455–67.

45 Hombrink P, Raz Y, Kester MGD, *et al*. Mixed functional characteristics correlating with TCR-ligand koff -rate of MHC-tetramer reactive T cells within the naive T-cell repertoire. *Eur J Immunol* 2013;43:3038–50.

46 van Bergen CAM, van Luxemburg-Heijs SAP, de Wreede LC, *et al*. Selective graft-versus-leukemia depends on magnitude and diversity of the alloreactive T cell response. *J Clin Invest* 2017;127:517–29.

47 Marijt WAE, Heemskerk MHM, Kloosterboer FM, *et al*. Hematopoiesis-restricted minor histocompatibility antigens HA-1- or HA-2-specific T cells can induce complete remissions of relapsed leukemia. *Proc Natl Acad Sci U S A* 2003;100:2742–7.

48 Yewdell JW. Confronting complexity: real-world immunodominance in antiviral CD8+ T cell responses. *Immunity* 2006;25:533–43.

49 de Witte M, Daenen LGM, van der Wagen L, *et al*. Allogeneic Stem Cell Transplantation Platforms With Ex Vivo and In Vivo Immune Manipulations: Count and Adjust. *Hemasphere* 2021;5:e580.

50 Penack O, Marchetti M, Aljurf M, *et al*. Prophylaxis and management of graft-versus-host disease after stem-cell transplantation for haematological malignancies: updated consensus recommendations of the European Society for Blood and Marrow Transplantation. *Lancet Haematol* 2024;11:e147–59.